

OPTIMIZATION OF A-TIG WELDING PARAMETERS FOR IMPROVING WELD GEOMETRY OF AISI 304L STAINLESS STEEL BY TAGUCHI APPROACH

Ganesh S Mudaliyar¹, Priyank B Patel², J.D. Patel³, Ayesha M Doi⁴

¹P.G. Student, Department of Production Engineering, M.E.C, Mehsana- 384315, Gujarat, India

² Assistant Professor, Department of Mechanical Engineering, M.I.T, Mehsana- 384315, Gujarat, India

³ Assistant Professor, Department of Mechanical Engineering, M.I.T, Mehsana- 384315, Gujarat, India

⁴ Lecturer, Department of Mechanical Engineering, G.P. Himatnagar-383001, Gujarat, India

ABSTRACT

Gas tungsten arc welding (GTAW) welding has an inherent difficulty in achieving deep penetration. The depth of penetration that can be achieved in 6mm thick S. S plate with conventional GTAW welding is approx. 2.5 mm which can be enhanced by silicon dioxide flux. The aim of the research work is to identify the effect of silicon dioxide flux on weld geometry and analyse it. Silicon dioxide flux plays a major role in influencing the various properties of stainless steel GTAW welds. Input parameters of GTAW mainly welding speed, current, Arc frequency etc. have been taken to find out the effect of input parameters on weld bead geometry. However, investigation is based on Taguchi method to determine the influence of process parameter and to optimize them.

Keyword: - Activated-TIG welding, Depth of penetration, Weld bead width, Flux, Angular distortion, Stainless Steel 304L.

1. INTRODUCTION

The study was concerned with the activating flux gas tungsten arc welding. The flux ingredient, which is inorganic compound (which can be used to produce deep penetration and arc constriction) are available in variety of range and compositions. Some of fluxes have been reported effective for particular materials. Activating fluxes contain oxides and halides (chlorides and fluorides). Oxide coating consists of iron, chromium, silicon, titanium, manganese, nickel, cobalt, molybdenum and calcium are reported to improve weld ability and increase the welding speed. The halogens, calcium fluoride and AlF_3 , have claim to constrict the arc and increase weld depth of penetration activated flux is a mixture of inorganic material suspended in volatile medium (acetone, ethanol etc).

In activated flux GTAW process as shown in figure 2, a thin layer of the fine flux is applied on the surface of the base metal with brush before welding. Flux mixed with acetone to make it in a paste form as shown in the figure 1. During activated flux, welding a part or all the fluxes is molten and vaporized. There is different types of fluxes (oxides) used in welding like MnO_2 , SiO_2 , TiO_2 , MoO_3 , and Al_2O_3 etc. As a result, the penetration of the weld bead is significantly increased.

Gas tungsten arc welding (GTAW) welding has an inherent difficulty in achieving deep penetration. The depth of penetration that can be achieved in 86mm thick S.S plate with conventional GTAW welding is approx. 2.5 mm which can be enhanced by silicon dioxide flux. The aim of the research work is to identify the effect of silicon dioxide flux on weld geometry and analyses it. Silicon dioxide flux plays a major role in influencing the various properties of stainless steel GTAW welds.

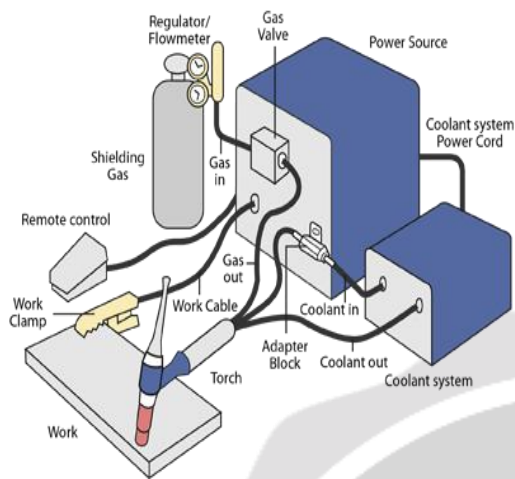


Fig -1: Schematic of TIG welding set up

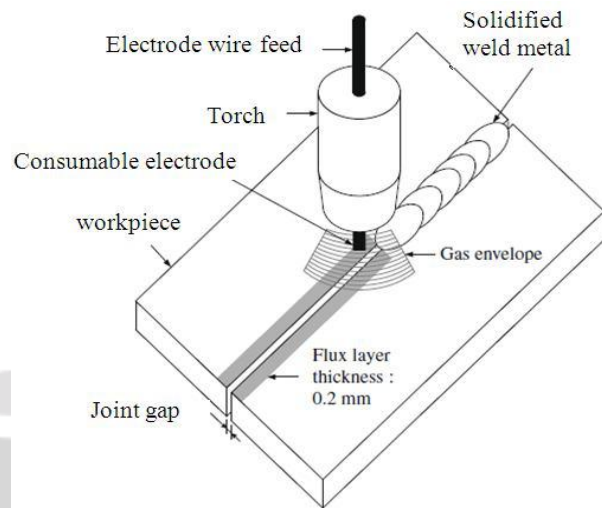


Fig -2: Schematic of A-TIG welding [10]

1.1 Mechanism of A-TIG Welding

Available literatures show that some of the mechanisms, which play major role in increase weld quality are Marangoni Effect, Buoyancy force, Electromagnetic force, Arc constriction due to active flux, Arc constriction due to negative ions. Arc concentration effect is explained in Figure 3. As the surface flux evaporates and surrounded by a region of arc as atoms which forms under the high temperature of weld arc. Evaporated atoms seize electrons and shape into the negative ion in the region due to lower temperature inside. Arc conductivity decreased the automatic contraction and the heat concentrated. This concentrated arc permits control of heat input to the work piece resulting in a narrow heat affected zone. This is an advantage because while this process is ongoing, the base metal faces change due to superheating of arc and fast cooling rate.

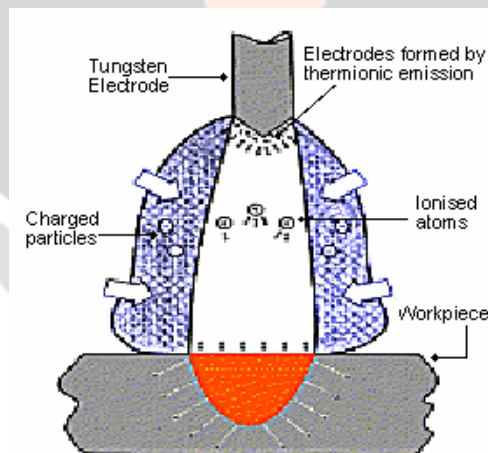


Fig -3: Mechanism of arc constriction due to vaporized molecules [2]

2. EXISTING LITERATURE REVIEW

Kurtulmus M et al. (2017) had studied the parameters are welding current, welding speed and flow rate on depth of penetration. In this review paper, A-TIG welding of austenitic stainless steels is examined. The effects of the activated flux welding mechanisms, the flux chemical composition, thickness of the flux, flux powder size welding

current, the arc voltage, the arc length, the welding speed and composition of the shielding gas on weld geometry of austenitic stainless-steel a-TIG welds are explained in detail. When the oxygen concentration in the weld metal is over 70 wt. ppm, the Marangoni convection in the weld pool changes from outward to inward. Consequently, a deep and narrow weld shape forms. A-TIG welding process leads to less welding distortions and higher weld strengths. Deep welds give distinguished savings in welding time and weld costs.

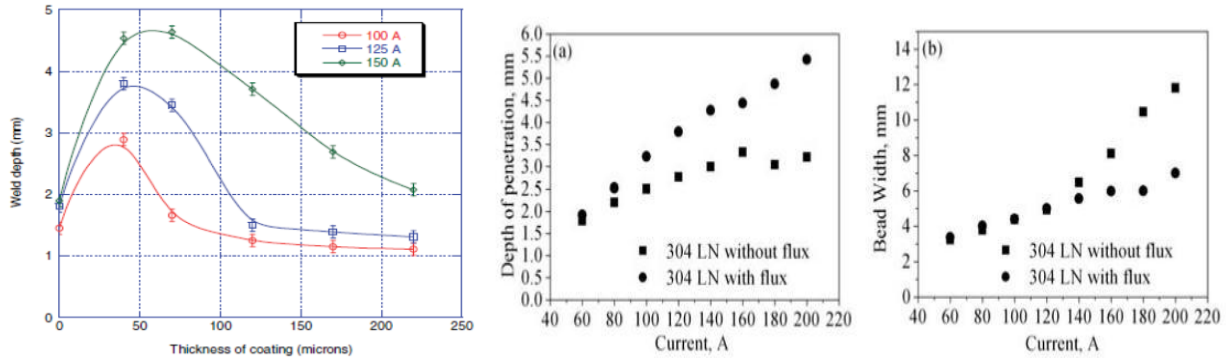


Fig -4: Penetration depths and bead width with coating thickness in A-TIG welding [2]

Babu A. V. Santhana et al. (2016) had examined penetration capability of tungsten inert gas (TIG) process, flux bounded TIG (FBTIG) in aluminum alloy aa 2219 t87. The bead depth is also observed as 1.91mm in conventional TIG process where as the depth significantly improved to 4.61mm in FBTIG process. When peak pulse current is varied from 160 to 240A, the bead depth increases steadily from 1.04 to 3.04mm. The depth to width ratio increases from 0.24 to 0.34 as the peak current increases from 160 to 220A. When current increases further to 240 A, the ratio slightly decreases to 0.33. This is because along with depth, bead width also increases at current levels above 220A.

Kumar V et al. (2016) had presented research on effect of TIG welding parameters such as welding current, gas flow rate, welding speed, weld torch angle that are influences on responsive output parameters such as weld penetration, width, fusion area, micro hardness, and tensile strength of welding using taguchi method. Surface plots and perturbation plot are generated by using mathematical models developed for penetration, weld width, fusion area and UTS these plots may be useful for prediction of the responses like UTS, penetration, width and fusion area the response can also be estimated from these plots. Hardness value increased from base region to HAZ and HAZ to weld region.

Kumar G et al. (2016) had studied bead-on-plate welds were made on 10-mm-thick 304b plates using gas tungsten arc welding with Ar and Ar+2% nitrogen as the shielding gases, activated-flux GTA and electron-beam welding processes. By using variable input parameters defect-free welds of 304b4 borated stainless steels can be easily made using GTA, activated-flux GTA, nitrogen-added GTA and EB welding processes.

Vasudevan M et al. (2016) had developed flux for enhancing the penetration performance of TIG welding process for autogenous welding of type 304L and 316L stainless steels. Multi-component activated flux was developed which was found to increase penetration of 10-12 mm in single-pass TIG welding of type 304L and 316L S.S. Improvement in toughness. Values were observed in 316L stainless steel produced by A-TIG welding due to refinement in the weld microstructure in the region close to the weld center. This research also compares 304L (10-mm-thick) stainless steel weld joints made by TIG and A-TIG welding processes.

Patel et al. (2014) conducted the tests on sheets with the dimensions of 100×70×6 mm were prepared and tests were conducted. Optimal parameters of the process are welding current 110 A, gas flow rate 13 l/min, at constant TiO₂ flux. And for SiO₂ flux the optimal parameter of the process are welding Current 110 A, gas flow rate 7 l/min, for using the proportion flux the optimal process parameter are welding current 110 A, gas flow rate 7 l/min and flux proportion are 60 % SiO₂ AND 40% TiO₂ flux. Weld penetration depth is increased in due to the increase in the current and it was also determined that decrease the weld width which is important term of welding distorting.

Alsabti et al. (2014) concluded that mainly arc temperature and arc force contributed to the deeper weld penetration using two designed flux-cored tubular wires containing cryolite (Na_3AlF_6) and MgF_2 . Immersion corrosion test

results on the ATIG weld specimens in separate 3.5% sodium chloride and 0.1% phosphoric acid solutions for 800 h, particularly in terms of mass loss, compared favorably with the autogenous welds. Wires 45 and 15 produced welds with much better corrosion resistance than TI-CP G2. As the cryolite content in the flux increases, the weld penetration, arc force, and arc temperature increase as well.

Tseng et al. (2010) had used input parameters as activated flux (MnO_2 , TiO_2 , MoO_3 , and Al_2O_3), weld current-200A, travel speed-150mm/min, diameter of electrode-3.2mm, tip angle of electrode 45° , electrode gap- 2mm, shielding gas-pure argon and gas flowrate -10 l/min which is used to analyses impact on weld morphology, angular distortion, delta-ferrite content, and hardness of type 316l stainless steels using optical microscope. When using oxide fluxes, the delta-ferrite content in activated TIG weld metal slightly increased to 7.0–7.6 FN. This result showed that type 316l stainless steel TIG welding with SiO_2 flux produced a substantial increase in the weld depth and weld depth-to-width ratio of about 7.25mm and 1.02. Constricted arc plasma as a mechanism in increasing activated TIG penetration.

3. EXPERIMENTAL SETUP

The chemical composition of SS 304 which is selected for experiment is provided in the table below:

Material	C	Si	S	P	Mn	Ni	Cr	Mo
Stainless steel AISI 304	0.061	0.350	0.007	0.034	1.110	8.010	18.280	0.260

Table -1: Chemical composition (wt %) of stainless steel 304L

Based on the literature review of past researcher and studying the range available in Lorch V50 is selected, number of levels and their values are shown in Table 2, so in this experiment 3 factors L18 level Taguchi design is performed.

Sr.No	INPUT PARAMETER	LEVEL 1	LEVEL 2	LEVEL 3	UNIT	Sr.No	OUTPUT FACTOR
1	Welding current	160	170	180	Ampere	1	Weld bead width(mm)
2	Arc pulse frequency	1	2	3	Hertz	2	Angular distortion($^\circ$ Degree)
3	Travel speed	65	85	-	mm/min	3	Depth of penetration(mm)

Table -2: Input & Output Process Parameters

3.1 Gas Tungsten Arc Welding Machine Set Up

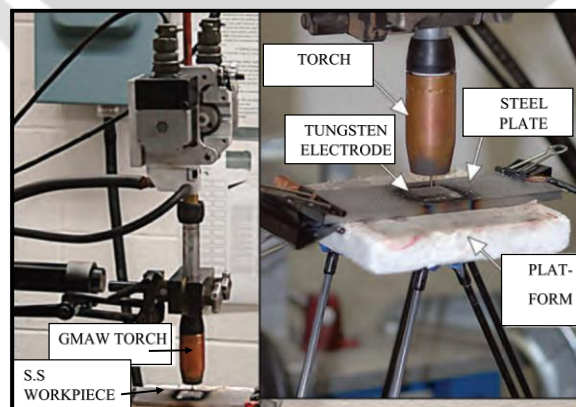


Fig -5: Working of TIG Welding Machine With its setup

(Source: Keepsake welding research institute center of excellence, L.D college of engineering)

Before welding, SiO₂ Flux is mixed with acetone with the ratio of 1:1 having 0.2mm thickness of layer and is applied on S.S 304L welding specimen.



Fig -6: Method of applying flux powder

3.2 Measurement of Output parameters

3.2.1 Depth of penetration and Weld Bead width

After welding, the cross-sections of the welded seams were prepared by standard metallographic procedures, such as sectioning, polishing and etching. In sectioning, samples were cut into size of 50x20mm from welded pieces to measure weld bead profile. After that polishing was done on all the samples with the help of emery papers. After using abrasive paper, Velvet Cloth and Alumina Powder were also used for getting reflecting surface. After that specimen are ready for etching operation. Etching is done to highlight the weld bead and identify microstructure feature or phases present. Specimen was dipped into the etchant for two minutes. The exothermic reaction takes place results in revealing the weld bead of the sample. The sample was immediately washed under running water and dried with air blower. After proper etching of the specimen, the weld bead and depth of penetration got visible using stereo Zoom microscope.

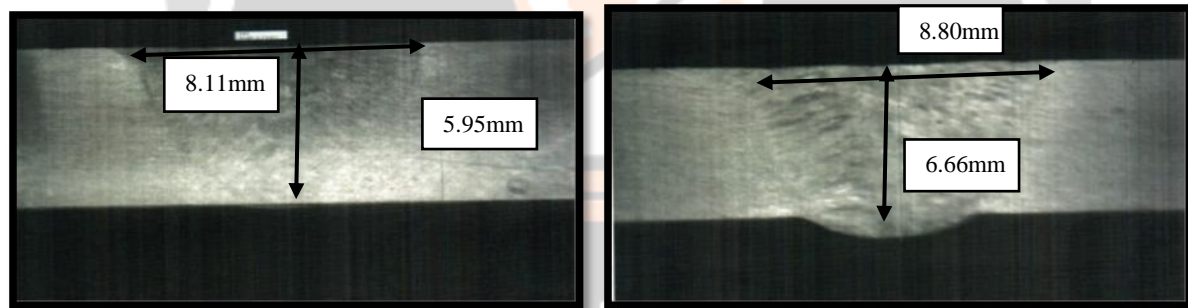


Fig -7: Weld Geometry at Travel speed 65mm/min & 85mm/min, welding current 180A & 160A and Pulse Frequency 2Hz & 3Hz.

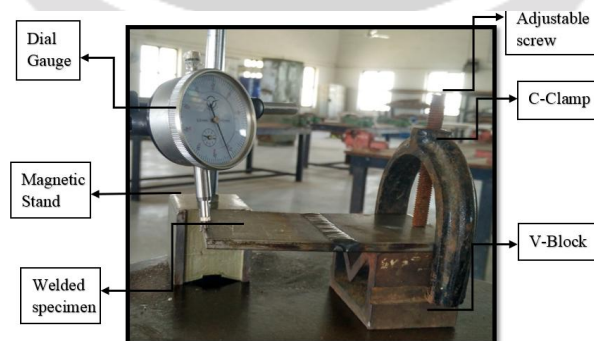


Fig -8: Experimental View of Angular Distortion Measurement

4. RESULTS, ANALYSIS AND DISCUSSION

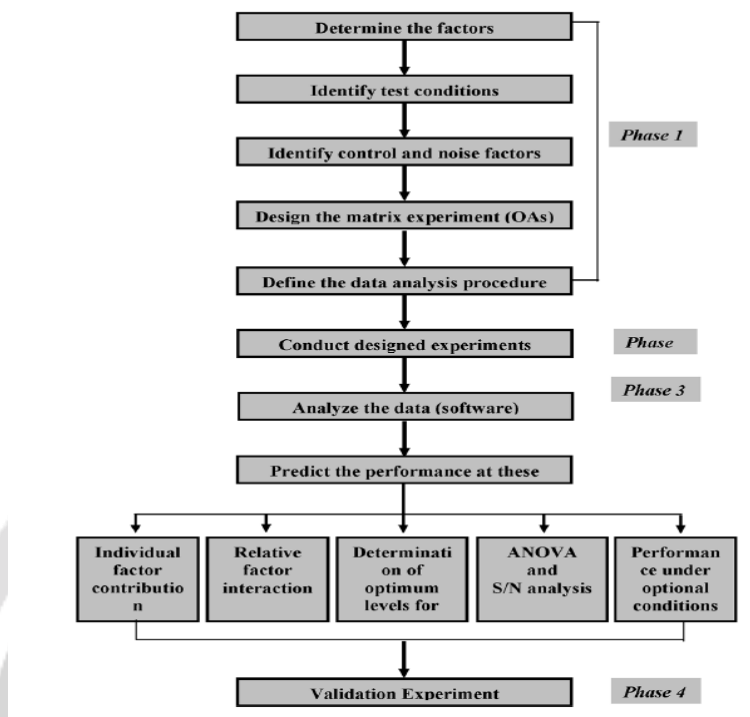


Fig -9: Steps involved in the use of Taguchi methodology

4.1 Experiment results by S/N analysis

Ex No	Welding Speed (mm/min)	Arc Pulse Frequency (Hz)	Welding current (Amp)	Weld Penetration (mm)	Weld Bead width (mm)	Angular Distortion (Degree)	S/N of weld penetration	S/N of weld bead width	S/N of Angular Distortion
1	65	1	160	6.29	8.35	1°52	15.9730	-18.4337	-3.63687
2	65	1	170	6.06	8.32	1°33'14"	15.6495	-18.4025	-2.47703
3	65	1	180	6.66	7.80	1°22'19"	16.4695	-17.8419	-1.72720
4	65	2	160	5.99	8.80	2°37'48"	15.5485	-18.8897	-6.31941
5	65	2	170	5.57	8.36	1°57'09"	14.9171	-18.4441	-3.91799
6	65	2	180	5.95	8.11	1°55	15.4903	-18.1804	-3.80663
7	65	3	160	6.32	9.09	2°08'08"	16.0143	-19.1713	-4.50619
8	65	3	170	6.43	8.12	1°50'	16.1642	-18.1911	-3.52183
9	65	3	180	6.78	7.55	1°30'56"	16.6246	-17.5589	-2.27887
10	85	1	160	6.17	8.77	2°03'21"	15.8057	-18.8600	-4.24375
11	85	1	170	5.74	8.32	1°44'	15.1782	-18.4025	-3.16725
12	85	1	180	6.84	7.88	1°32'39"	16.7011	-17.9305	-2.41148
13	85	2	160	5.94	9.10	2°21'24"	15.4757	-19.1808	-5.84512
14	85	2	170	4.86	8.58	2°11'28"	13.7327	-18.6697	-4.95947
15	85	2	180	6.21	8.10	2°07'39"	15.8618	-18.1697	-4.45433
16	85	3	160	5.66	9.37	2°02'24"	15.0563	-19.4348	-5.84512
17	85	3	170	5.59	8.58	2°05'55"	14.9482	-18.6697	-4.40216
18	85	3	180	6.26	8.22	1°54'	15.9315	-18.2974	-3.75041

Table -3: S/N analysis after applying flux

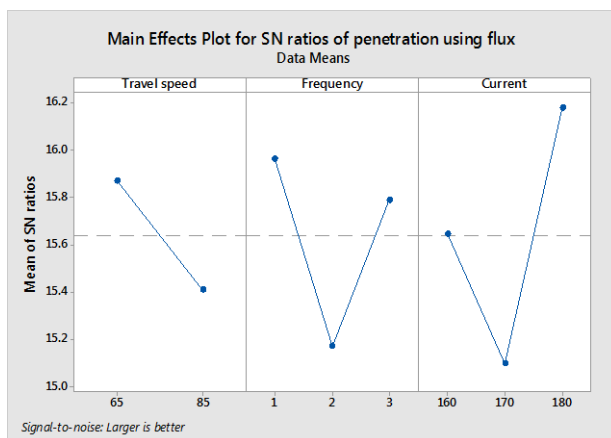


Fig -10: Main effects plot for S/N ratio of penetration.

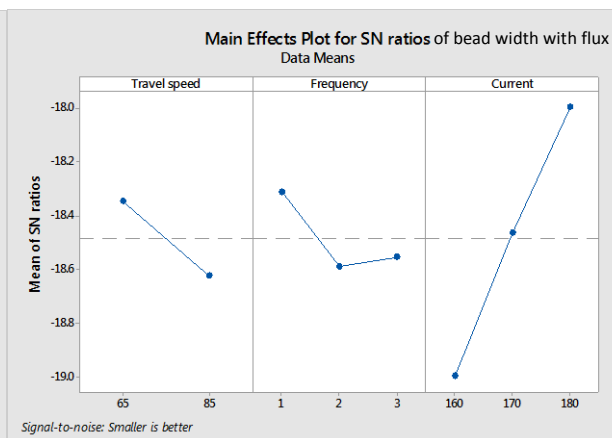


Fig -11: Main effects plot for S/N ratio of penetration.

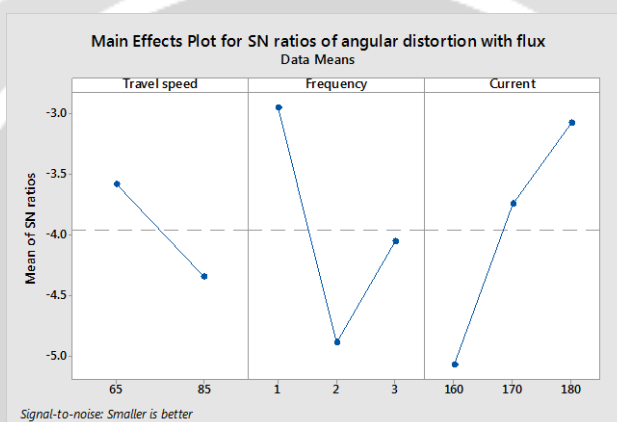


Fig -12: Main effects plot for S/N ratio of penetration.

4.2 Analysis of Variance with flux

Analysis of variance (ANOVA) is a statistical method to analyses variation in a response variable (continuous random variable) measured under conditions defined by various factors (classification variables, often with nominal levels). Frequently, we use ANOVA to test equality among various means by comparing variance among groups relative to variance within groups (random error).

Based on the above discussion, the optimal welding process parameters are arc current at level 2, welding speed at level 2, and welding arc frequency at level 2. The effects of arc voltage and preheat temperature are negligible. Therefore, experiment 9 shown in Table 3 fits the optimal process conditions.

1) Analysis of penetration with flux

Source	DF	Adj SS	Adj MS	F-Value	P-Value	Percent. Cont.
Travel speed	1	0.4294	0.42936	5.34	0.039	10.70%
Frequency	2	0.9648	0.48240	6.00	0.016	24.05%
Current	2	1.6514	0.82572	10.27	0.003	41.17%
Error	12	0.9648	0.08040			
Total	17	4.0104				

Based on the analysis of the S/N ratio the highest penetration is obtained for welding current of 180A (level 3), Arc pulse frequency 1Hz (level 1) and travel speed of 85 mm/min (level 2). Based on ANOVA of depth of penetration, it can be concluded that current play a major role of 41.17% during welding with flux.

2) Analysis of bead width with flux

Source	DF	Adj SS	Adj MS	F-Value	P-Value	Percent. Cont.
Travel speed	1	0.3254	0.32536	7.88	0.016	8.29%
Frequency	2	0.2681	0.13407	3.25	0.075	6.83%
Current	2	2.8320	1.41602	34.32	0.000	72.23%
Error	12	0.4952	0.04126			
Total	17	3.9207				

Based on the analysis of the S/N ratio the highest penetration is obtained for welding current of 180A (level 3), Arc pulse frequency 3Hz (level 3) and travel speed of 65 mm/min (level 1). Based on ANOVA of bead width, it can be concluded that current play a major role of 72.33% during welding with flux.

3) Analysis of angular distortion with flux

Source	DF	Adj SS	Adj MS	F-Value	P-Value	Percent. Cont.
Travel speed	1	0.08134	0.081339	14.85	0.002	8.48%
Frequency	2	0.37954	0.189772	34.64	0.000	39.58%
Current	2	0.43221	0.216106	39.45	0.000	45.07%
Error	12	0.06573	0.005478			
Total	17	0.95883				

Based on the analysis of the S/N ratio the highest penetration is obtained for welding current of 180A (level 3), Arc pulse frequency 3Hz (level 3) and travel speed of 65 mm/min (level 1). Based on ANOVA of depth of penetration, it can be concluded that current play a major role of 45.07% and frequency consists of 39.58% during welding with flux.

4.3 Confirmation Experiments

Experiments were conducted based on optimal levels in order to get best results. The level chosen for this experiment are travel speed 65 mm/sec, Arc frequency 3 Hz and welding current 180 A.

Exp No.	Travel Speed mm/sec	Arc frequency Hz	Welding current Amp	Depth of penetration mm	Bead width mm	Angular distortion Degree
1	65	3	180	6.71	7.67	1°41'54"
2	65	3	180	6.57	7.52	1°34'

Table-4: Confirmation experiments for best result.

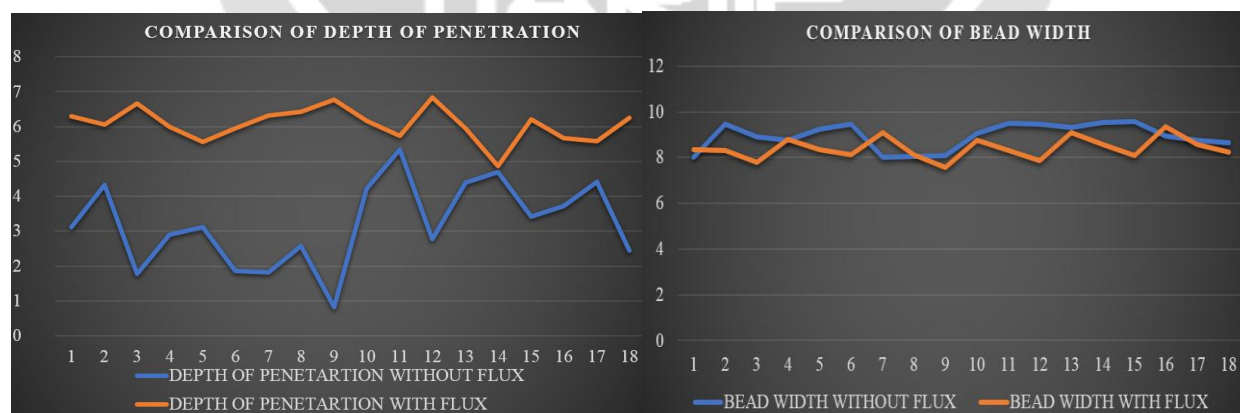


Fig -13: Comparison of depth of penetration

Fig -14: Comparison of bead width

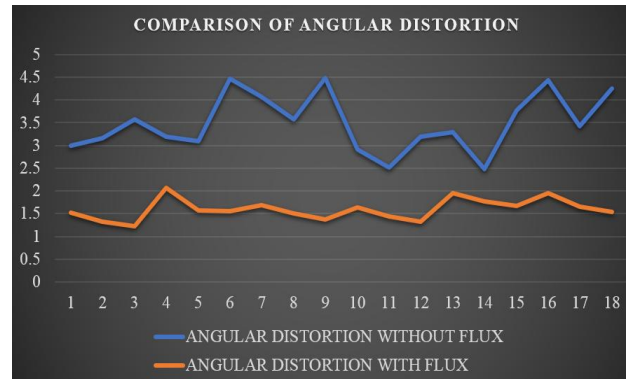


Fig -15: Comparison of angular distortion

Fig-13 depicts that the penetration is more with flux powder as compared to penetration without flux powder. With comparing these two experiments, 47.20% improvements have been noticed penetration with flux powder.

Fig-14 depicts that the bead width will reduce with flux powder as compared to bead width without flux powder. With comparing these two, 5.8 % reduction have been noticed bead width with flux powder.

Fig-15 depicts that the angular distortion has been reduced with flux powder as compared to angular distortion without flux powder. With comparing these two, 54.08 % reduction have been noticed angular distortion with flux powder.

5. CONCLUSIONS

The model was optimized using ANOVA with MINITAB18 software. Experimental validations of the model are also performed. Various conclusions obtained were:

- Best result of weld penetration, bead width and angular distortion are found which is 6.78mm, 7.55 mm and 1°30'56" respectively.
- Experiments were conducted based on optimal levels in order to get best results. The optimal level chosen for this experiment are travel speed 65 mm/sec, Arc frequency 3 Hz and welding current 180 A. Optimum value of depth of penetration is 6.78mm, bead width is 7.55 and angular distortion is 1°30'56".
- ANOVA will provide the best optimization which is quite fast.
- F-value and p-value shows that all the factors are significant.
- Increasing Welding current & Arc frequency increases the penetration.
- Arc frequency plays a major role in influencing the angular distortion on which limited research is available.
- ANOVA and TAGUCHI has given optimum result at lowest value of Travel speed and highest value of Welding current & Arc frequency.

6. ACKNOWLEDGEMENT

I would like to thank, J.D.Patel (Assistant Professor) & Priyank B Patel (Assistant Professor) Merchant Institute of Technology, Piludara, India providing research guidance and for their consistent help in writing this research paper. After that I reverently thanks to Ayesha M Doi (lecturer) Government polytechnic Himatnagar, India for their kind blessings regarding to my post-graduation.

7. REFERENCES

- [1] Agrawal Neha, Thakur Meenakshi, Raj Janmit & Baghel Anand "A Review on TIG/MIG Welded Joints", International Journal of Science Technology & Engineering, Vol. 4,2017,65-71.
- [2] Memduh Kurtulmus, Mustafa Kemal Bilici, Zarif catalgol, İrfan calis "Activated Flux TIG Welding of Austenitic Stainless Steels", Journal of Scientific and Engineering Research, Vol. 4,2017,169-177.

- [3] Babu A. V. Santhana, Giridharan P. K., Narayanan P. Ramesh and Murty S.V.S. Narayana "Prediction of Bead Geometry for Flux Bounded TIG Welding of AA 2219-T87 Aluminum Alloy" , Journal of Advanced Manufacturing Systems, Vol. 15, 2016,69-84.
- [4] Kumar Vijander "Parametric Study of Gas Tungsten Arc Welding on Mechanical Properties of Low Carbon Steel", International Journal for Scientific Research & Development, Vol. 5,2016,1222-1226.
- [5] Kumar Guttikonda Raja, Gabbita Durga Janaki Ram & Rao Sajja Rama Koteswara "Effect of activated flux and nitrogen addition on the bead geometry of borated stainless-steel GTA welds", Materials and technology 50, Vol. 3,2016, 357-364.
- [6] M.Vasudevan "Effect of A-TIG Welding Process on the Weld Attributes of Type 304LN and 316LN Stainless Steels", Journal of Materials Engineering and Performance, Vol. 3,2016,239-242.
- [7] Duhan Ravi & Choudhary Suraj "Effect of different fluxes on hardness and microstructure of SS 304 in GTAW welding", International Journal of Mechanical Engineering (IJME), Vol. 3,2014,1-8.
- [8] Patel.Akash.B. and Prof. Patel.Satyam.P "The effect of activating fluxes in TIG welding by using Anova for SS 321", International Journal of Engineering Research and Applications, Vol. 4,2014,41-48.
- [9] Alsabti.T., Alshawaf .A., And Liu.S "Flux Assisted Gas Tungsten Arc and Laser Welding of Titanium with Cryolite Containing Fluxes: Arc Spectroscopy and Corrosion Resistance Studies", Welding Journal American Welding Society, Vol. 93, 2014,379-387.
- [10] Kuang-Hung Tseng, Chih-Yu Hsu "Performance of activated TIG process in austenitic stainless-steel welds", Journal of Materials Processing Technology, Vol.11,2010,503-512.
- [11] Qing-ming LI , WANG Xin-hong, ZOU Zeng-da, WU Jun "Effect of activating flux on arc shape and arc voltage in tungsten inert gas welding", Transactions of Nonferrous Metals Society of China, Vol. 17,2007,486-490.
- [12] Huang Her-Yueh "Effects of shielding gas composition and activating flux on GTAW weldments", Materials and Design, Vol. 30,2008,2404-2409.
- [13] Juang S.C., Tarng Y.S "Process parameter selection for optimizing the weld pool geometry in the tungsten inert gas welding of stainless steel", Journal for materials processing and technology, Vol. 122,2002,33-37.
- [14] Liu Liming, Zhang Zhaodong, Song Gang and Shen Yong "Effect of Cadmium Chloride Flux in Active Flux TIG Welding of Magnesium Alloys", Materials Transactions, Vol. 47,2006,446-449.
- [15] Narayanan Arun, Cijo Mathew, Baby Vinod Yeldo & Joseph Joby "Influence of Gas Tungsten Arc Welding Parameters in Aluminium 5083 Alloy". International Journal of Engineering Science and Innovative Technology (IJESIT), Vol. 2,2013,269-277.